

Histone deacetylase 1: a target of 9-hydroxystearic acid in the inhibition of cell growth in human colon cancer

Natalia Calonghi,^{1,*} Concettina Cappadone,^{*} Eleonora Pagnotta,^{*} Carla Boga,[†] Carlo Bertucci,[§] Jessica Fiori,[§] Gianluca Tasco,^{**} Rita Casadio,^{**} and Lanfranco Masotti^{*}

Department of Biochemistry G. Moruzzi,^{*} Department of Organic Chemistry A. Mangini,[†] Department of Pharmaceutical Sciences,[§] and Centro Interdipartimentale per le Ricerche Biotecnologiche Laboratory of Biocomputing,^{**} University of Bologna, Bologna, Italy

Abstract Recent studies have shown that an endogenous lipoperoxidation product, 9-hydroxystearic acid (9-HSA), acts in colon carcinoma cells (HT29) as a growth inhibitor by inducing p21^{WAF1} in an immediate-early, p53-independent manner and that p21^{WAF1} is required for 9-HSA-mediated growth arrest in HT29 cells. It is conceivable, therefore, to hypothesize that the cytostatic effect induced by this agent is at least partially associated with a molecular mechanism that involves histone deacetylase 1 (HDAC1) inhibition, as demonstrated for sodium butyrate and other specific inhibitors, such as trichostatin A and hydroxamic acids. Here, we show that, after administration, 9-HSA causes an accumulation of hyperacetylated histones and strongly inhibits the activity of HDAC1. The interaction of 9-HSA with the catalytic site of the enzyme has been highlighted by computational modeling of the human HDAC1, using its homolog from the hyperthermophilic *Aquifex aeolicus* as a template. Consistent with the experimental data, we find that 9-HSA can bind to the active site of the protein, showing that the inhibition of the enzyme can be explained at the molecular level by the ligand-protein interaction.—Calonghi, N., C. Cappadone, E. Pagnotta, C. Boga, C. Bertucci, J. Fiori, G. Tasco, R. Casadio, and L. Masotti. **Histone deacetylase 1: a target of 9-hydroxystearic acid in the inhibition of cell growth in human colon cancer.** *J. Lipid Res.* 2005. 46: 1596–1603.

Supplementary key words endogenous lipid peroxidation products • tumor • mass spectrometry • computational modeling

9-Hydroxystearic acid (9-HSA) belongs to the class of endogenous lipid peroxidation by-products that are greatly diminished in tumors and therefore become unable to exert their normal controlling functions on cell division (1). Indeed, in HT29 cells, exogenous administration of 9-HSA at micromolar concentrations results in a significant inhibition of proliferation rate as well as a significant increase of p53-independent p21^{WAF1} expression

(2). The expression of the cell cycle kinase inhibitor p21^{WAF1} is induced in neoplastic cells by histone deacetylase 1 (HDAC1) inhibitors such as phenyl butyrate, sodium butyrate, trichostatin A (TSA), and suberoylanilide hydroxamic acid (SAHA). Increased expression of p21^{WAF1} may play a critical role in the growth arrest induced in transformed cells by these agents, and it can be regulated, at least in part, by histone acetylation of the chromatin associated with the *p21^{WAF1}* gene. Histone acetylation and gene activation induced by HDAC1 inhibitors would consequently be selective (3). The mode of action of 9-HSA is similar to that of HDAC inhibitors.

Crystallographic studies performed using TSA and SAHA indicate that these compounds inhibit HDAC activity by interacting with the catalytic site, thereby blocking substrate access (4, 5). Short-chain fatty acids, such as phenyl butyrate and phenyl acetate, inhibit HDAC activity and affect the expression of numerous genes with disparate cellular functions (6–8). These agents have been tested in the clinic, but they suffer from a short plasma half-life as well as from the relatively high (millimolar) concentrations that are required for their action. On the other hand, hydroxamic acids such as TSA, SAHA, *m*-carboxycinnamic acid bishydroxamic acid, and oxamflatin can be used at micromolar and nanomolar concentrations and generally have in vivo longer half-life and bioavailability than the short-chain fatty acids. The anticancer potential of HDAC inhibitors stems from their ability to affect several cell processes that are deregulated in neoplastic cells. For the most part, the activation of differentiation programs, inhibition of the cell cycle, and induction of apoptosis are the key antitumor activities of such molecules (3, 9). The remarkable tumor specificity of these compounds, and their potency in vitro and in vivo, underscore the potential of HDAC inhibitors as exciting new agents for the treatment of cancer (10, 11).

Manuscript received 26 October 2004 and in revised form 25 January 2005.

Published, JLR Papers in Press, February 16, 2005.
DOI 10.1194/jlr.M400424-JLR200

¹ To whom correspondence should be addressed.
e-mail: natalia.calonghi@unibo.it

Copyright © 2005 by the American Society for Biochemistry and Molecular Biology, Inc.

This article is available online at <http://www.jlr.org>

To date, the mode of action of 9-HSA on cancer cells has not been explored. Here, we have investigated whether the effects of 9-HSA on the proliferation of HT29 cells can be related to the inhibition of HDAC1 through a direct ligand-enzyme interaction.

MATERIALS AND METHODS

Synthesis of 9-HSA and 9-deutero-9-hydroxystearic acid

Methyl 9-oxooctadecanoate and methyl 9-hydroxyoctadecanoate were prepared according to the literature (12). ¹H- and ¹³C-NMR spectra were recorded on a Gemini 300 spectrometer (Varian, Palo Alto, CA) at 300 and 75.46 MHz, respectively. Chemical shifts were measured in δ , and, if not specified, referenced to CDCl₃ (7.27 ppm for ¹H-NMR and 77.0 ppm for ¹³C-NMR). *J* values are given in Hz. Signal multiplicities were established by Distortionless Enhancement by Polarization Transfer experiments. Mass spectrometry was performed using a VG-7070E spectrometer at an ionization voltage of 70 eV. Infrared (IR) spectra were recorded using a Perkin-Elmer FT-IR MOD.1600 spectrophotometer. Melting points were determined with a Buchi apparatus and are uncorrected. Silica gel, 230–400 mesh, and silica gel-coated plates (Kieselgel 60 F254) were purchased from Merck (Darmstadt, Germany) and were used for flash chromatography and TLC, respectively, the spots being developed with an aqueous solution of (NH₄)₆MoO₄ (2.5%) and (NH₄)₄Ce(SO₄)₄ (1%) in 10% H₂SO₄. Sodium borodeuteride was purchased from Sigma-Aldrich (Milan, Italy).

Methyl 9-deutero-9-hydroxyoctadecanoate (9-deutero-9-hydroxystearic acid methyl ester)

To a solution of methyl 9-oxooctadecanoate (0.200 g, 0.64 mmol) in methanol (10 ml), 0.05 g (1.28 mmol) of sodium borodeuteride was added. After stirring at room temperature for 6 h, the mixture was treated with water (2 ml) and extracted with ethyl acetate (3 × 5 ml). The organic layer was dried over anhydrous Na₂SO₄ and filtered, and the solvent was removed on a rotary evaporator. Flash chromatography of the residue (petroleum light/Et₂O, 7:3) gave 0.18 g (89.6%) of pure methyl 9-deutero-9-hydroxyoctadecanoate. Melting point, 49–51°C (from methanol). ¹H-NMR (CDCl₃): 3.67 (s, 3H, OCH₃), 2.30 (t, 2H, *J* = 7.4 Hz, CH₂COO), 1.62 (t, 2H, *J* = 7.4 Hz, CH₂CH₂COO), 1.55–1.15 (m, 27H, incl. OH), 0.88 (t, 3H, *J* = 6.6 Hz, CH₃). ¹³C-NMR (CDCl₃): 174.3, 71.5 (t, *J* = 21.4 Hz, C-D), 51.4, 37.4, 37.3, 34.1, 31.9, 29.7, 29.6, 29.56, 29.5, 29.3, 29.2, 29.1, 25.6, 25.5, 24.9, 22.7, 14.1. IR (CHCl₃): 3,389, 1,739 cm⁻¹. MS (*m/z*): 316 (M⁺ + 1), 298, 284, 265, 188, 156.

9-Hydroxyoctadecanoic acid (9-HSA)

A portion (0.200 g, 0.64 mmol) of methyl 9-hydroxyoctadecanoate was dissolved in 10% KOH/CH₃OH (4 ml) and stirred at room temperature overnight. The solvent was removed on a rotary evaporator, the residue was dissolved in water and extracted with ethyl acetate, and the organic layer was eliminated. The aqueous solution was treated with 6 N HCl until pH = 3–4, then was extracted with ethyl acetate. The organic layer was washed with “brine,” dried over anhydrous Na₂SO₄, filtered, and concentrated at reduced pressure. 9-HSA (0.16 g, 83%) was obtained. Melting point, 77–79°C (from methanol) (13): 76–77°C. ¹H-NMR: 12.00–10.50 (b.s., 1H, COOH), 3.60–3.53 (m, 1H, CHOH), 2.35 (t, 2H, *J* = 7.5 Hz, CH₂COO), 1.50–1.20 (m, 27H, incl. OH), 0.87 (t, 3H, *J* = 6.8 Hz, CH₃). ¹³C-NMR: 178.7, 72.0, 37.5, 37.4, 33.5, 31.9, 29.7, 29.6 (two signals), 29.4, 29.3, 29.2, 29.0, 5.7,

25.5, 24.7, 22.7, 14.1. IR (CHCl₃): 3,427, 1,707 cm⁻¹. MS (*m/e*): 283, 282 (M⁺ – H₂O), 264, 155.

9-Deutero-9-hydroxyoctadecanoic acid (9-deutero-9-hydroxystearic acid)

This compound was prepared from 9-deutero-9-hydroxystearic acid methyl ester with the same procedure described for the preparation of 9-HSA. Melting point, 77–78°C (from methanol). ¹H-NMR (CDCl₃): 6.40–6.20 (b.s., 2H, COOH and OH, disappear after the addition of D₂O), 2.34 (t, 2H, *J* = 7.4 Hz, CH₂COO), 1.55–1.10 (m, 26H), 0.88 (t, 3H, *J* = 6.4 Hz, CH₃). ¹³C-NMR (CDCl₃): 179.4, 71.6 (t, *J* = 22.1 Hz, C-D), 37.3, 37.2, 34.0, 32.0, 29.7, 29.6 (two signals), 29.4, 29.3, 29.2, 29.0, 25.6, 24.6, 22.7, 14.1. IR (CHCl₃): 3,378, 1,711 cm⁻¹. MS (*m/e*): 284, 265, 156.

Cell culture and treatments

The colon cancer cell line HT29 was purchased from the American Type Culture Collection (Manassas, VA). HT29 cells were maintained in RPMI 1640 medium (Labtek Eurobio, Milan, Italy) supplemented with 10% fetal calf serum (Euroclone, Milan, Italy) and 2 mM L-glutamine (Sigma-Aldrich, St. Louis, MO) at 37°C and 5% CO₂. HT29 cells were seeded at 2 × 10⁴ cells/cm² in a plastic well (60 cm²) and allowed to grow for 1 day before being exposed to 100 μM 9-HSA or 9-deutero-9-hydroxystearic acid (9-HSA-d).

LC-electrospray ionization-MS and data analysis

The nuclei of HT29 cells treated for 2, 6, 12, 24, or 48 h with 9-HSA-d were extracted according to Amellem et al. (14). Nuclear lipids were extracted according to Folch, Lees, and Stanley (15). LC-MS analyses were performed on a PU-1558 liquid chromatograph (Jasco, Tokyo, Japan) interfaced with a LCQ Duo (ThermoFinnigan, San Jose, CA) mass spectrometer equipped with an electrospray ionization (ESI) source (4.5 eV) and operated with an Ion Trap analyzer. HPLC separation was carried out on a Waters XTerra™ MS C18, 3.5 μm (3.0 × 150 mm inner diameter) column using a mobile phase consisting of methanol-0.05% acetic acid in water (80:20, v/v) at a flow rate of 0.2 ml/min and an injection volume of 20 μl.

LC-MS analyses were conducted operating in both full scan and single ion monitoring (SIM) modes (negative polarity). The mass spectra were recorded over the *m/z* range 50–450 (3 microscans/s), providing the total ion current (TIC) chromatograms. SIM chromatograms were also obtained at *m/z* 300 [M – H]⁻, the base peak of the deuterated 9-HSA-d. Capillary temperature was 220°C. A calibration graph was obtained for the quantitative assay of deuterated 9-HSA-d. A standard solution of the hydroxy acid was prepared by dissolving the appropriate weight of the pure substance in methanol to obtain a final concentration of 43.2 mM. Standard solutions for the calibration graph construction were prepared by diluting appropriate volumes of the working standard with mobile phase to give final concentrations of 0.86, 4.32, 8.64, 14.4, and 21.6 μM. Deuterated 9-HSA solutions were analyzed (SIM mode) by 20 μl loop injections, and the linearity of the response was checked before each deuterated 9-HSA quantitative assay.

Preparation of [³H]acetyl histones

To obtain [³H]acetyl-labeled histones as the substrate for the HDAC assay, 1 × 10⁷ HT29 cells were incubated in 30 ml of medium containing 0.5 mCi/ml [³H]acetate for 1 h, cultured with or without 100 μM 9-HSA for 6 h, and the labeled histone fraction was immediately extracted. Cells were harvested using 0.11% trypsin and 0.02% EDTA, washed twice with 10 mM sodium butyrate in PBS, and nuclei were isolated according to Amellem et al. (14). Sodium butyrate (5 mM) was added to nu-

clear isolation buffer to prevent histone deacetylation. The nuclear pellet was suspended in 0.1 ml of ice-cold water using a Vortex mixer, and concentrated H₂SO₄ was added to the suspension to give a final concentration of 0.4 N. After incubation at 4°C for 1 h, the suspension was centrifuged for 5 min at 14,000 g, and the supernatant was taken and mixed with 1 ml of acetone. After overnight incubation at -20°C, the coagulate material was collected by microcentrifugation and air-dried. This acid-soluble histone fraction was dissolved in 50 µl of water. Proteins were quantified using a protein assay kit (Bio-Rad, Hercules, CA).

Immunoprecipitation of HDAC1

The nuclei of HT29 cells were isolated, and the nuclear pellet was suspended in HDA buffer (20 mM Tris-HCl, pH 8.0, 150 mM NaCl, 10% glycerol, 10 µg/ml each of aprotinin, leupeptin, pepstatin, and antipain, and 0.5 mM *p*-amidinophenol methanesulfonylfluoride), sonicated, and then centrifuged at 12,000 g for 20 min at 4°C. The protein concentration of the extracts was determined using a protein assay kit (Bio-Rad). A sample containing 500 µg of protein was incubated overnight at 4°C with 5 µg of anti-HDAC1 polyclonal antibody (Upstate Biotechnology, Lake Placid, NY) in HDA buffer. Fifty microliters of protein A-Sepharose (50%, v/v; Amersham, Uppsala, Sweden) was added to each sample, incubated for 1 h, centrifuged at 12,000 g for 20 min at 4°C, and finally washed four times with HDA buffer, pH 8.0. Samples were then divided for assay of deacetylase activity against [³H]acetate-labeled HT29 histones and for electrophoresis and Western blotting analysis against HDAC1.

Assay for HDAC activity

Immunoprecipitates were incubated with [³H]acetate-labeled HT29 histones (12,000 dpm/2 µg) for 2 h at 37°C. HDAC1 inhibitory activity of 9-HSA was estimated in 50 µl of a reaction mixture containing immunoprecipitated HDAC1, [³H]acetate-labeled HT29 histones (12,000 dpm), and 5 µM 9-HSA dissolved in HDA buffer at 37°C for 2 h. The reaction was stopped by the addition of 50 µl of 1 M HCl and 0.16 M acetic acid. The released [³H]acetic acid was extracted with 0.5 ml of ethyl acetate, and the solvent layer was taken into 5 ml of toluene scintillation solution for the determination of radioactivity. Histones were extracted from HT29 cells (both control and treated with 9-HSA) and examined by 15% SDS-PAGE and Western blot analysis against acetylated lysines using anti-acetylated lysine (Cell Signaling Technology, Beverly, MA).

Mass spectrometry

The procedure for in-gel digestion originally developed by Shevchenko et al. (16) was used with some modifications. Briefly, Coomassie Blue-stained bands were excised from the gel and washed with 100 mM ammonium bicarbonate and acetonitrile, reduced with DTT at 56°C for 45 min, and then alkylated by iodoacetamide in the dark for 30 min. The gel was incubated in 50 µl of a 12 ng/µl trypsin solution in 50 mM ammonium bicarbonate, pH 8.0, and incubated at 4°C for 1 h. Then, the supernatant was removed and fresh buffer was added to cover gel pieces during the enzymatic cleavage at 37°C overnight. The resulting peptides were extracted first with a 1:1 solution of 25 mM ammonium bicarbonate and acetonitrile and then with a 1:1 solution of 5% formic acid and acetonitrile.

The extracted tryptic peptides were lyophilized and resuspended with 10 µl of 0.2% trifluoroacetic acid (TFA) for Matrix Assisted Laser Desorption Ionization-MS (Voyager-DE PRO; Applied Biosystems). One microliter was mixed with 1 µl of a solution of α -cyano-4-hydroxycinnamic acid in CH₃CN, 0.1% TFA was applied (10 mg/ml), and the mixture was loaded on the stainless-steel sample target. The sample and the matrix were al-

lowed to air-dry before spectra were collected. Mass spectra were generated from the sum of 50 laser shots. Spectra mass calibration was performed using trypsin autodigestion fragments and α -cyano-4-hydroxycinnamic acid dimmer as internal standards.

Homology modeling of HDAC1

The three-dimensional model of HDAC1 was modeled by comparison with the three-dimensional structure of an HDAC homolog from *Aquifex aeolicus*, bound to TSA [Protein Data Bank (PDB) code 1C3R], and known with a 0.2 nm resolution (4). Alignment of the target with the template was performed with CLUSTAL W (17), constraining the conservation of residues involved in metal coordination (Matrix Blosum 62) and gap penalty. The last 100 C-terminal residues of the template were excluded from the alignment, because the coverage with 1C3R is shorter than the actual sequence length of the target. Modeling was performed with the program Modeller 6.2 (18). For a given alignment, 10 model structures were built and were evaluated with the PROCHECK suite of programs (19).

Docking of 9-HSA with HDAC1

Molden (<http://www.cmbi.kun.nl/index.html>) was used to build the three-dimensional model of 9-HSA. The docked molecule was the charged form of 9-HSA to better mimic the environmental conditions at pH 8. Flexibility was constrained in C9, considering both the left and rectus enantiomers of the molecule. Flexible docking was performed with Autodock version 3.0, which allows flexible docking by means of a Lamarckian genetic algorithm (20). Fifty independent runs were performed, each one processing a population of 100 conformations for 27,000 generations, with rates of mutation and crossover set to 0.02 and 0.8, respectively. The elitism parameter was set to 2. The docked conformation with the lowest value of estimated free binding energy was retained for further analysis. To compute the parameters to be used in docking 9-HSA to HDAC1, the molecule was placed in the pocket overlapping the corresponding zinc-containing binding site in the template (1C3R), where TSA is bound.

Statistical analysis

In some cases, a paired Student's *t*-test was used to determine whether treated and untreated samples were significantly different. *P* < 0.05 was considered significant and evidence of population differences.

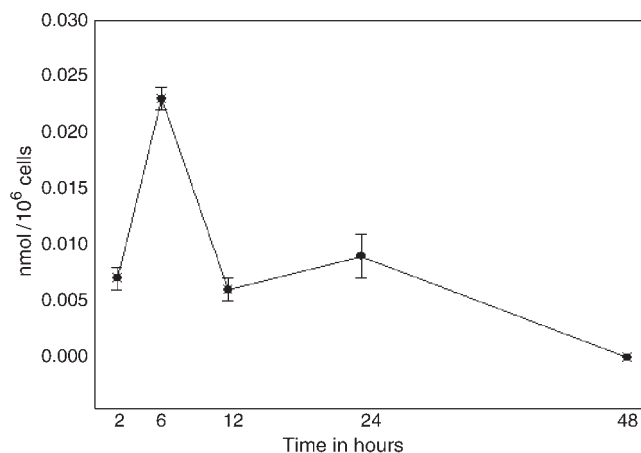


Fig. 1. Time course of 9-deutero-9-hydroxystearic acid (9-HSA-d) in HT29 nuclear lipid fractions for 48 h after dosing. Data points indicate means of three separate experiments \pm SD.

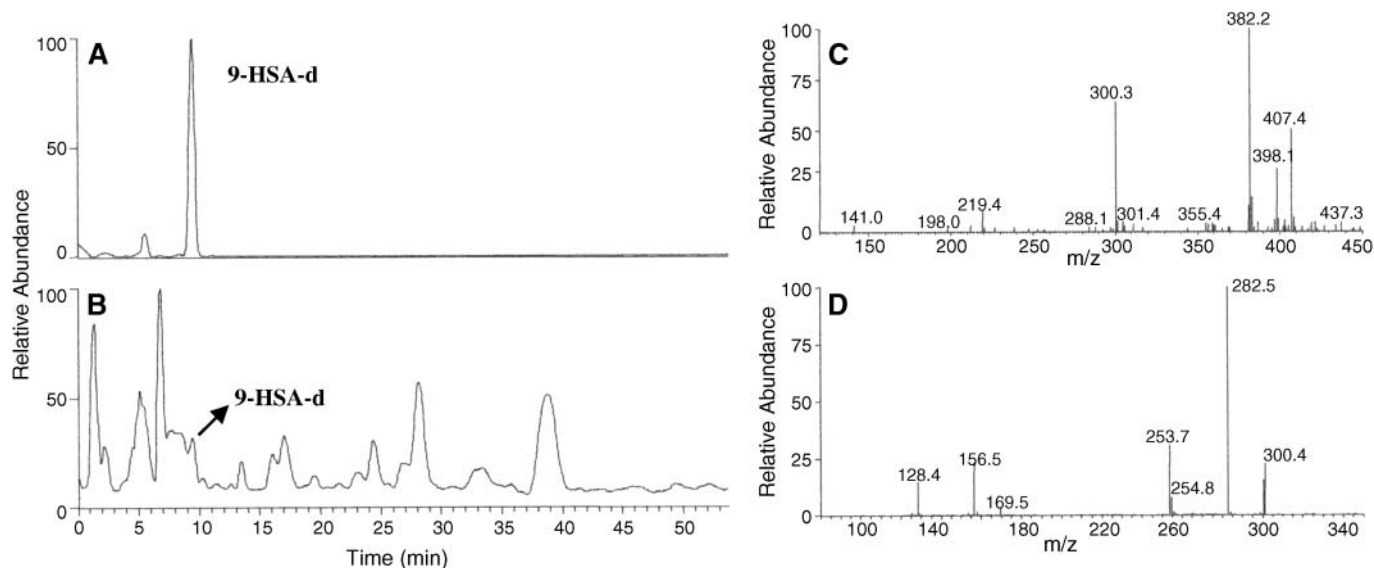


Fig. 2. Typical LC/MS chromatograms obtained for real-sample analysis of the content of treated nuclei. A: Single ion monitoring chromatogram at m/z 300. B: Total ion current chromatogram, m/z 50–450 mass range. C: MS spectrum of 9-HSA-d. D: MS/MS spectrum of the precursor ion at m/z 300.3. Chromatographic conditions were as follows: C18 column; mobile phase of methanol and 0.05% acetic acid in water (80:20, v/v); flow rate of 0.2 ml/min.

RESULTS

Synthesis of 9-HSA and 9-HSA-d

These compounds were synthesized by selective reduction with sodium borohydride and sodium borodeuteride, respectively, of methyl 9-oxooctadecanoate, followed by alkaline hydrolysis of the methyl ester with methanolic KOH solution.

Nuclear localization of 9-HSA

The concentration-time profile of 9-HSA-d in the HT29 nuclear fraction for 48 h after dosing is shown in **Fig. 1**. Nuclear lipids from HT29 cells exposed for 2, 6, 12, 24, or 48 h to 9-HSA-d were extracted, and LC/ESI/MS analysis was performed as described. The y axis units are expressed as nanomoles of 9-HSA-d per 10^6 cells. 9-HSA-d nuclear concentration reached a maximum at 6 h and declined below the limit of detection at 48 h.

The mass spectra recorded in SIM and TIC chromatograms of the nuclear lipid fraction are shown in **Fig. 2A, B**, respectively. The TIC MS spectrum (**Fig. 2C**) and the MS/MS spectrum of the precursor ion at m/z 300.3 (**Fig. 2D**) were also acquired to confirm the peak identity. The quantitative assays were performed in SIM mode on the basis of a calibration graph.

HDAC activity is inhibited by 9-HSA

To assess HDAC activity, the nuclear proteins were immunoprecipitated and assayed using [3 H]acetyl histones as the substrate. The results in **Fig. 3** show that equivalent levels of HDAC in the reaction mixture resulted in a significant inhibition of enzyme activity in the presence of 9-HSA. HDAC1 enzymatic activity was monitored by measuring the amounts of [3 H]acetic acid released from the [3 H]acetylated histones. As shown in **Fig. 3**, 5 μ M 9-HSA

inhibited \sim 66.4% of the enzyme activity. **Figure 4A** shows the profiles of histones extracted from HT29 cells, control and treated, and separated by 15% SDS-PAGE. The addition of 9-HSA to the cell culture resulted in the accumula-

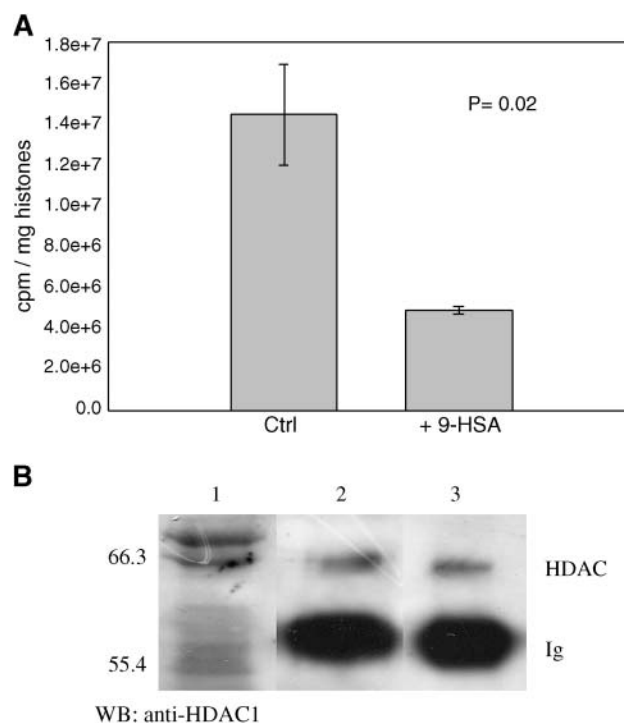


Fig. 3. Effect of 9-hydroxystearic acid (9-HSA) on histone deacetylase 1 (HDAC1) activity. HDAC1 was IP, and immunocomplexes were divided and assayed for deacetylase activity against [3 H]acetyl-labeled HT29 histones (upper) and analyzed by anti-HDAC1 Western blot (lane 1, protein marker; lanes 2, 3, with and without 9-HSA) (lower). Enzyme activity is expressed as cpm/mg histone. Reported values represent means \pm SD of six independent experiments ($P = 0.02$). Ctrl, control.

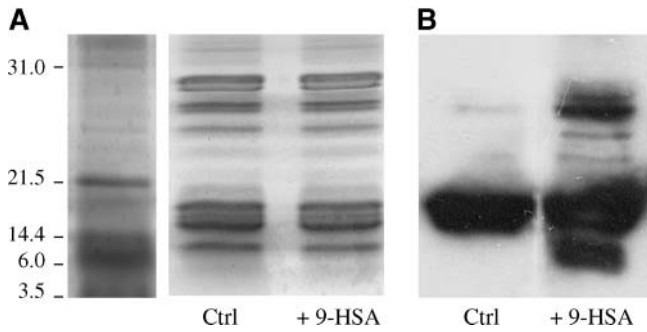


Fig. 4. Hyperacetylation of nuclear histones caused by 9-HSA. A: Histones were stained by Coomassie Blue to reveal the amount of histones loaded on the blots. B: The histones were isolated from nuclei of control and treated HT29 cells, analyzed by 15% SDS-PAGE, and immunoblotted with antibody specific for acetylated lysine. Ctrl, control.

tion of acetylated histones in total cellular chromatin (Fig. 4B). In particular, the band at 10 kDa corresponding to histone H4 MW was more acetylated in treated cells than in control cells.

Mass spectrometry analysis

Mass spectrometry was used to evaluate the effect of 9-HSA treatment on histone H4 acetylation. The bands at

10 kDa of control and 9-HSA-treated cells by 15% SDS-PAGE were excised and subjected to enzymatic digestion by trypsin. The resulting peptide mixtures were analyzed by MALDI/time of flight (Fig. 5), and the obtained mass spectra were used both to confirm the identity of the protein and to characterize the acetylation sites.

Many molecular masses corresponding to theoretical tryptic peptides of histone H4 were detected in both spectra, allowing the identification of the digested protein with certainty. In addition, signals at m/z 877.218 and 1,240.6715 were observed only in the spectrum of the protein from treated cells; these values did not match any canonic peptide from the protein, whereas they exactly corresponded to the molecular masses of the peptide 9-16 acetylated at the ϵ -amino group of Lys-12 and the peptide 1-8 acetylated at the ϵ -amino group of Lys-5. This finding led to the identification of this amino acid as one of the hyperacetylation sites of histone H4 after 9-HSA cell treatment.

Can we explain these data at the molecular level?

The molecular interaction of 9-HSA with the HDAC was investigated by a computational approach. First, a model of the protein was computed using homology building. A histone deacetylase homolog, solved at atomic resolution, was present in the PDB database of structures (3). The identity of the human sequence with the homolog was

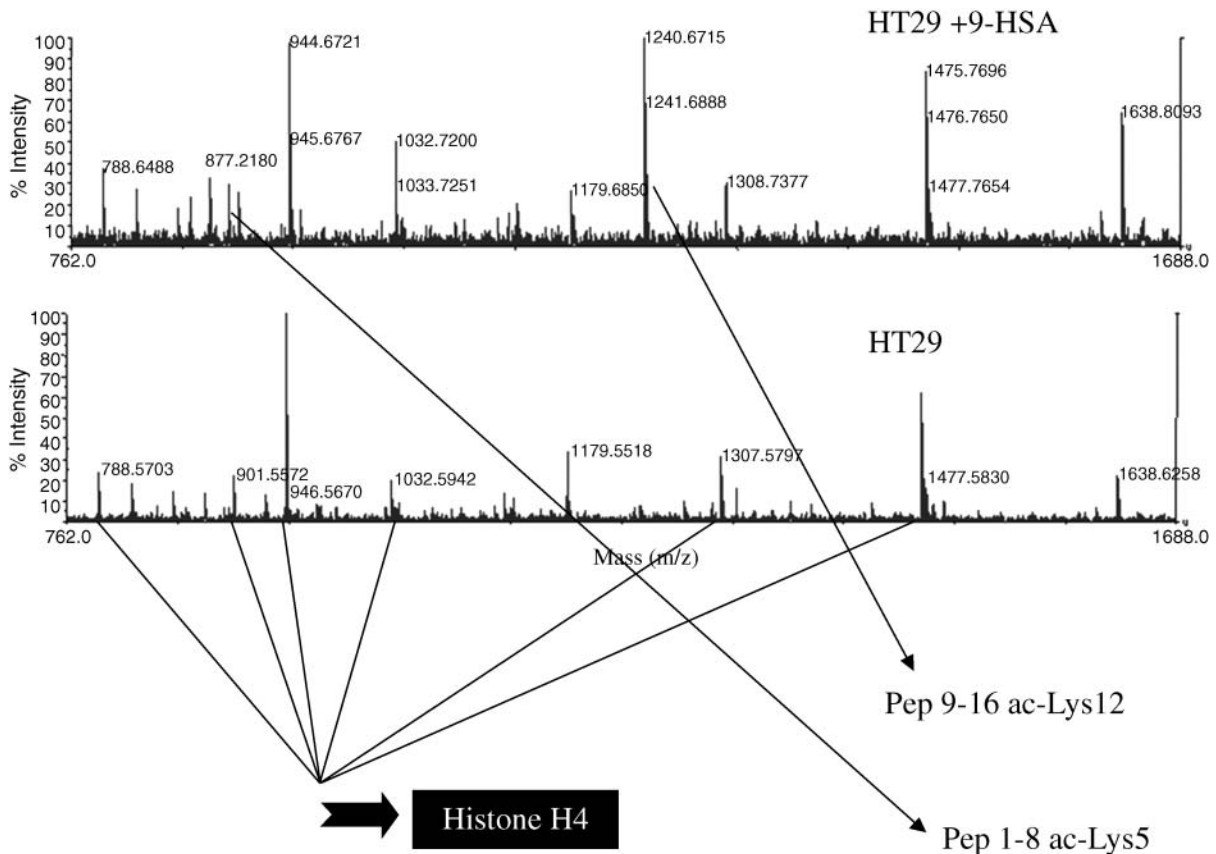


Fig. 5. MALDI-time of flight spectra of histone H4 digested by trypsin. MS analysis of in-gel tryptic digest of histone H4 bands isolated by 15% SDS-PAGE from histone extract of control and 9-HSA-treated cells. The signals at m/z 877.218 and 1,240.6715, corresponding to the molecular masses of peptide 9-16 acetylated on Lys-12 and peptide 1-8 acetylated on Lys-5, were observed only in the spectrum of protein from treated cells.

A

```

PDB          -----KKVKLIGTLDYGKYRYPKNHPLKI PRVSL LRFK DAMNLI DEKEL IKS RPAT 52
HDA1_HUMAN  MAQTQGTTRKVCYYDGDVGNYYGQGHPMKPHRIRMTNLLNLYGLYRKMEIYRPHKAN 60
           : **      * * * * : * * * * * * : : : : * : * : : : * .

PDB          KEELLLFHTEDYINTLMEAEERSQSVKPGAREKYNIGGYE-NPVSYAMFTGSSLATGSTVQ 111
HDA1_HUMAN  AEEMTKYHSDDYIKFLRSIRPDNMSEYSKQMRQFNVG-EDCPVFDGLFEFCQLSTGGSSVA 119
           ** : : * : * : * : * . . : : : : * * * * . : * . : * : * : *

PDB          AIEEFLKG--NVAFN PAGGMHAFKSRANGF CYINNP AVGIEYL RKKGFKRILYI D L D A N 169
HDA1_HUMAN  SAVKLNKQQTDI AVNWAGGLHAKKSEASGFCYVNDIVLAI LLELLKY-HQRVLYI D I I H 178
           : : : * : : * * * : * * * * * * * * * * * * : : . * * * . : * : * * * : *

PDB          HCDGVQEA FYD TDQV FVLS LHQS PEYAF PFEKGFLEE IGE GK GKY N L N I P L P K G L N D N E 229
HDA1_HUMAN  HGDGVVEA FYT T D R V M T V S F H K Y G E Y - F P - G T G D L R D I G A G K G Y A V N Y P L R D G I D D E S 236
           * * * * : * * * * * * * : : * : * : * * * * * * * * * * * * * * * * : * * * * : * : * .

PDB          FLFALEKSL EIVKEVFEPEVYLLQLGTDPLLEDYLSKFNLSNVAFLKAFNIVREVFGEV 289
HDA1_HUMAN  YEAI FKPVMSKVMHEMFP S A V V L Q C G S D L S G D R L G C F N L T I K G H A K C V E F V K S F N L P M L 296
           : : : : * * * * * * : * * * * * * * * * * * * * * * * * * * * * * * * * * * * * * * * * *

PDB          YLGGGGYHPYALARAUTLIWCELSGREVPEKLNKAKE LLKS ID FEE FDDEVD RSYMLET 349
HDA1_HUMAN  MLGGGGY T I R N V A R C W T Y E T A V A L D T E I P N E L P Y N D Y F E Y F G P D F K L H I S P S N M T N Q M T N 356
           * * * * * * * : * * * * * . * : * : * * : : * * * * . . : : : .

PDB          LKDPWRGGEVRKEVKDTLEKAKA----- 372
HDA1_HUMAN  EYLEKIKQRLFENLRMLPHAPGVQMQAIPEDAIPPEESGDEDEDDPKRISICSSDKRIAC 416
           : : : : : . . . .

PDB          -----
HDA1_HUMAN  EEEFSDSEEEGEGGRKNSNFKAKRVKTEDEKEKDP E E K K V T E E E K T K E E K P E A K G V K 476
PDB          -----
HDA1_HUMAN  EEVKLA 482

```

Active site coordinating the Zn ion
Residues relevant in the stabilisation of the active

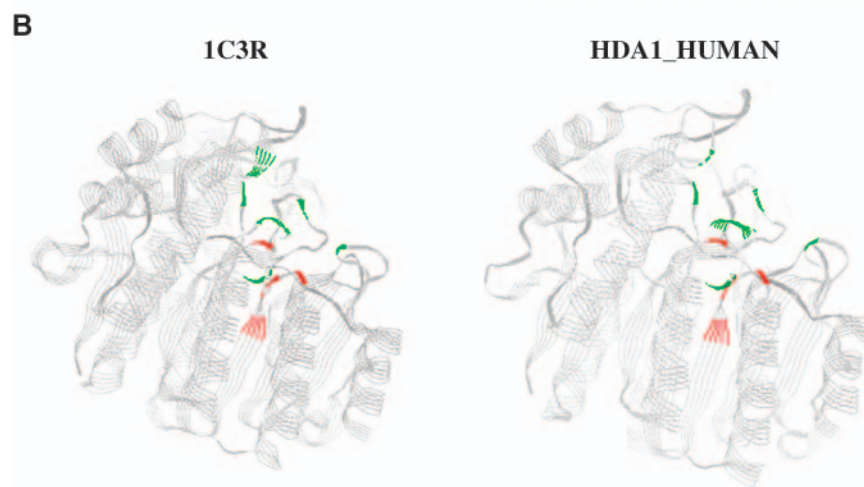


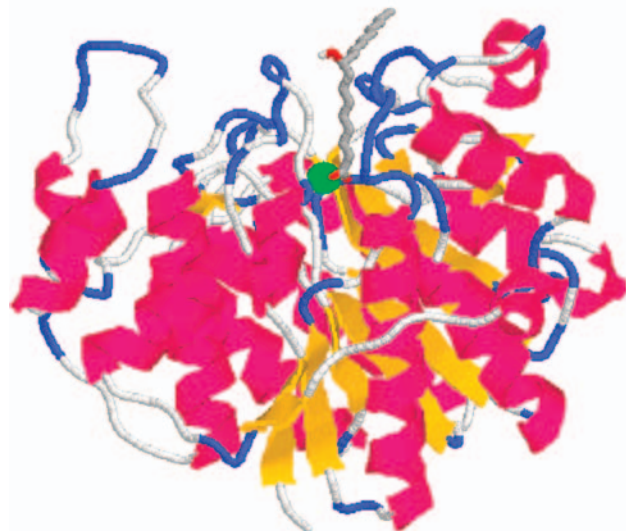
Fig. 6. Alignment between the target sequence (HDAC1_HUMAN) and the template [Protein Data Bank (PDB) code 1C3R] with a sequence identity of 31.4% (upper). The four residues of the active site (H170, D166, D168, and D256) are shown in red; residues stabilizing the active sites (P21, G90, H132, H133, G141, F142, F197, L263, and Y295) are shown in green. The last 103 residues in the C-terminal part of the protein (~20% of the whole sequence) are not modeled because they do not have any counterpart in the target (lower).

greater than 30%, and building by homology could be applied. The alignment between the target sequence and the template is shown in **Fig. 6** (upper), where residues known to interact with TSA in the zinc ion-dependent binding site of the known structure from *A. aeolicus* are also highlighted. Indeed, although the global level of homology of the two chains was low, it is evident that residues interacting with the ligand were conserved. Our analysis overall confirmed previous observations in the literature (3) and prompted us to create a three-dimensional model for the human chain using building by homology. The model is shown in **Fig. 6** (lower). The computed model was rather similar to the original template (Root Mean Square Deviation = 0.4 Å) and similarly

belongs to the α/β class, according to the Structural Classification of Proteins classification (<http://scop.mrc-lmb.cam.ac.uk/scop/data/scop.b.d.e.j.b.c.b.html>). The C-terminal portion of the chain was not modeled, because the template can structurally cover only 375 residues. Like the template, the modeled fragment contained 12 α -helices and 8 β -strands. The folding of the binding site in the model was well conserved with respect to the template. Zinc ion, as also predicted from sequence alignment, was coordinated to residues Asp-166, Asp-168, His-170, and Asp-256 (**Fig. 6**, lower).

The protein-ligand interaction was characterized with a docking procedure. To simulate the physiological environment, both the *R* and *S* enantiomeric forms of 9-HSA

A



B

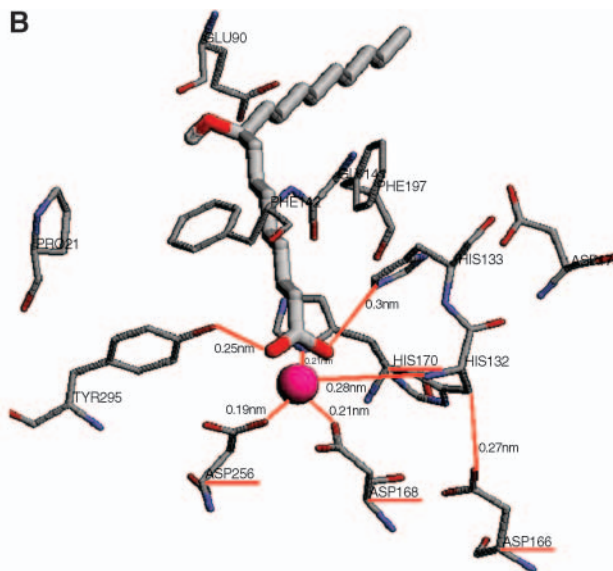


Fig. 7. A: Docking of 9-HSA to zinc-dependent human HDAC1. The zinc ion is shown in green (spacefill), and 9-HSA is shown in wireframe. The protein is shown in cartoon. The graphic representation is obtained with RasMol. B: The active site of HDAC1. The residues involved in zinc binding and the active site are shown in red (H160, D166, D168, and D256).


were docked in a flexible way to the zinc ion-dependent binding site. The binding of 9-HSA is rather similar to that of TSA in the template: the molecule interacts with conserved residues in the ion-containing pocket: Pro-21, Glu-90, His-132, His-133, Gly-141, Phe-142, Asp-173, Phe-197, and Tyr-295 (Fig. 6, upper, and Fig. 7A, B).

DISCUSSION

Recent studies have demonstrated that the administration of 9-HSA to HT29 cells induces a proliferative arrest mediated by direct activation of the p21^{WAF1} gene, bypassing p53 (2). These data correlate with the biological activities of the HDAC inhibitors, which can reactivate gene expression and inhibit the growth and survival of tumor cells (10). Six hours after administration to HT29 cells, the nuclear content of 9-HSA was maximal; therefore, the histone hyperacetylation was investigated at this time. The accumulation of the hyperacetylated histones was more evident in the case of histone H4 (Fig. 4B). The histone H4 acetylation was further followed by mass spectrometry, demonstrating that the protein is modified on Lys-5 and Lys-12 (Fig. 5). The enzymatic activity assay showed that 9-HSA inhibited ~66.4% of the HDAC1 activity in vitro. The molecular interaction of 9-HSA with HDAC1 was finally investigated with a computational approach, demonstrating that the binding of 9-HSA to the active site of HDAC1 was rather similar to that of TSA.

Recently, the crystal structure of an HDAC-like protein from the hyperthermophilic *A. aeolicus* (PDB code 1C3R) bound to the HDAC inhibitors TSA and SAHA was reported (4). We performed the three-dimensional modeling of HDAC1 by using this homolog as a template. Such a procedure affords an active site of the human enzyme sim-

ilar to that of its homolog, characterized by seven loops with a coordinated zinc ion. The interaction of 9-HSA with the catalytic site of the model has been tested with a docking procedure. Consistent with the experimental results, we find that 9-HSA can bind to the active site of the three-dimensional model of the human protein, confirming that a possible explanation of our results at the molecular level is the ligand-enzyme interaction. Notably, when interacting with the site, the *R*-9 enantiomer is more stable than the *S* enantiomer; in fact, the energy of interaction is -8.45 and -1.97 kcal/mol for the *R* and *S* isomers, respectively, and the estimated free energy of binding is -6.31 and $+4.98$ kcal/mol for the *R* and *S* forms, respectively. Furthermore, the fact that an unnatural *S* enantiomer of TSA is totally inactive suggests the involvement of a target molecule with strict stereospecificity (21, 22).

In conclusion, we clearly indicate that the endogenous lipoperoxidation product 9-HSA is an inhibitor of HDAC1 and that its effects on cancer cell proliferation and differentiation can be attributed to the inhibition of the enzyme. 

This work was supported by grants from Ministero dell'Istruzione e della Ricerca (60% 2003, COFIN 2002).

REFERENCES

- Masotti, L., E. Casali, N. Gesmundo, G. Sartor, T. Galeotti, S. Borrello, M. Piretti, and G. Pagliuca. 1988. Lipid peroxidation in cancer cells: chemical and physical studies. *Ann. NY Acad. Sci.* **551**: 47–58.
- Calonghi, N., C. Cappadone, E. Pagnotta, G. Farruggia, F. Buontempo, C. Boga, G. L. Brusa, M. A. Santucci, and L. Masotti. 2004. 9-Hydroxystearic acid upregulates p21^{WAF1} in HT29 cancer cells. *Biochem. Biophys. Res. Commun.* **314**: 138–142.

3. Richon, V. M., T. W. Sandhoff, R. A. Rifkind, and P. A. Marks. 2000. Histone deacetylase inhibitor selectively induces p21^{WAF1} expression and gene-associated histone acetylation. *Proc. Natl. Acad. Sci. USA*. **97**: 10014–10019.
4. Finnin, M. S., J. R. Donigian, A. Cohen, V. M. Richon, R. A. Rifkind, P. A. Marks, R. Breslow, and N. P. Pavietich. 1999. Structures of histone deacetylase homologue bound to the TSA and SAHA inhibitors. *Nature*. **40**: 188–193.
5. Khochbin, S., A. Verdell, C. Lemerrier, and D. Seigneurin-Barny. 2001. Functional significance of histone deacetylase diversity. *Curr. Opin. Genet. Dev.* **11**: 162–166.
6. Lee, H. J., M. Chun, and K. V. Kandror. 2001. Trp60 and HDAC7 interact with the endothelin receptor A and may be involved in downstream signalling. *J. Biol. Chem.* **276**: 16597–16600.
7. Fischlee, W., V. Kiermer, F. Dequiecit, and E. Vercin. 2001. The emerging role of class II histone deacetylases. *Biochem. Cell Biol.* **79**: 337–348.
8. Davie, J. R. 2003. Inhibition of histone deacetylase activity by butyrate. *J. Nutr.* **133** (Suppl.): 2485–2492.
9. Sambucetti, L. C., D. D. Fischer, S. Zabludoff, P. O. Known, H. Chamberlin, N. Trogani, H. Xu, and D. Cohen. 1999. Histone deacetylase inhibition selectively alters the activity and expression of cell cycle proteins leading to specific chromatin acetylation and antiproliferative effects. *J. Biol. Chem.* **274**: 34940–34947.
10. Marks, P. A., R. A. Rifkind, V. M. Richon, R. Breslow, T. Miller, and W. K. Kelly. 2001. Histone deacetylase and cancer: causes and therapies. *Nat. Rev.* **1**: 194–202.
11. Johnstone, R. W. 2002. Histone deacetylase inhibitors: novel drugs for the treatment of cancer. *Nat. Rev.* **1**: 287–299.
12. Bertucci, C., M. Hudaib, C. Boga, N. Calonghi, C. Cappadone, and L. Masotti. 2002. Gas chromatography/mass spectrometric assay of endogenous cellular lipid peroxidation products: quantitative analysis of 9- and 10-hydroxystearic acids. *Rapid Commun. Mass Spectrom.* **16**: 859–864.
13. Cochrane, C. C., and H. J. Harwood. 1961. Phase properties of mixtures of 9- and 10-oxo-octadecanoic acids and of 9- and 10-hydroxy-octadecanoic acids. *J. Org. Chem.* **26**: 1278–1282.
14. Amellem, O., T. Stokke, J. A. Sandvik, and E. O. Pettersen. 1996. The retinoblastoma gene product is reversibly dephosphorylated and bound in the nucleus in S and G2 phases during hypoxic stress. *Exp. Cell Res.* **227**: 106–115.
15. Folch, J., M. Lees, and G. H. S. Stanley. 1957. A simple method for the isolation and purification of total lipids from animal tissues. *J. Biol. Chem.* **226**: 497–509.
16. Shevchenko, A., M. Wilm, O. Worm, and M. Mann. 1996. Mass spectrometric sequencing of proteins from silver stained polyacrylamide gels. *Anal. Chem.* **68**: 850–858.
17. Thompson, J. D., D. G. Higgins, and T. J. Gibson. 1994. CLUSTAL W: improving the sensitivity of progressive multiple sequence alignment through sequence weighting, position-specific gap penalties and weight matrix choice. *Nucleic Acids Res.* **22**: 4673–4680.
18. Marti-Renom, M. A., A. Stuart, A. Fiser, R. Sánchez, F. Melo, and A. Sali. 2000. Comparative protein structure modeling of genes and genomes. *Annu. Rev. Biophys. Biomol. Struct.* **29**: 291–325.
19. Laskowski, R. A., M. W. MacArthur, D. S. Moss, and J. M. Thornton. 1993. PROCHECK: a program to check the stereochemical quality of protein structures. *J. Appl. Crystallogr.* **26**: 283–291.
20. Morris, G. M., D. S. Goodsell, R. S. Halliday, R. Huey, W. E. Hart, R. K. Belew, and A. J. Olson. 1998. Automated docking using a Lamarckian genetic algorithm and empirical binding free energy function. *J. Comput. Chem.* **19**: 1639–1662.
21. Yoshida, M., M. Kijima, M. Akita, and T. Beppu. 1990. Potent and specific inhibition of mammalian histone deacetylase both *in vivo* and *in vitro* by trichostatin A. *J. Biol. Chem.* **265**: 17174–17179.
22. Yoshida, M., Y. Hoshikawa, K. Koseki, K. Mori, and T. Beppu. 1990. Structural specificity for biological activity of trichostatin A, a specific inhibitor of mammalian cell cycle with potent differentiation-inducing activity in Friend leukemia cells. *J. Antibiot.* **43**: 1101–1106.